

SupMAE: Supervised Masked Autoencoders Are Efficient Vision Learners

Feng Liang¹ Yangguang Li² Diana Marculescu¹

¹The University of Texas at Austin ²SenseTime Research

{jeffliang, dianam}@utexas.edu liyangguang@sensetime.com

Abstract

Recently, self-supervised Masked Autoencoders (MAE) (He et al. 2021) have attracted unprecedented attention for their impressive representation learning ability. However, the pre-text task, Masked Image Modeling (MIM), reconstructs the missing local patches, lacking the global understanding of the image. This paper extends MAE to a *fully-supervised* setting by adding a supervised classification branch, thereby enabling MAE to learn global features from golden labels effectively. The proposed Supervised MAE (SupMAE) only exploits a visible subset of image patches for classification, unlike the standard supervised pre-training where all image patches are used. Through experiments, we demonstrate that SupMAE is not only more training efficient, but it also learns more robust features. Specifically, SupMAE achieves comparable performance with MAE using only 30% of compute cost when evaluated on ImageNet with the ViT-B/16 model. SupMAE’s robustness on ImageNet variants and transfer learning performance outperforms MAE and standard supervised pre-training counterparts. Codes are available at <https://github.com/enyac-group/supmae>.

Introduction

Pre-training plays a crucial role in computer vision (CV). Supervised pre-training on ImageNet (Deng et al. 2009) and then transferring to downstream tasks (Girshick et al. 2014; Long, Shelhamer, and Darrell 2015; He et al. 2017) has revolutionized the entire community. While it works pretty well for convolutional neural networks (CNNs) (Krizhevsky, Sutskever, and Hinton 2012; Simonyan and Zisserman 2014; He et al. 2016), naive ImageNet supervised pre-training does not bring good performance for recently proposed vision transformers (ViT) (Dosovitskiy et al. 2020).

To unearth the potential of ViT, self-supervised pre-training methods (Chen*, Xie*, and He 2021; Caron et al. 2021; Bao, Dong, and Wei 2021; He et al. 2021; Xie et al. 2021b) are emerging as an alternative. Among them, the Masked Autoencoder (MAE) (He et al. 2021) is the state-of-the-art method that adopts a BERT-type masked autoencoding scheme (Devlin et al. 2018). As shown in the top part of Figure 1, MAE masks random patches of the input image and reconstructs the missing pixels with the visible patches. Although it achieves remarkable performance,

Copyright © 2024, Association for the Advancement of Artificial Intelligence (www.aaai.org). All rights reserved.

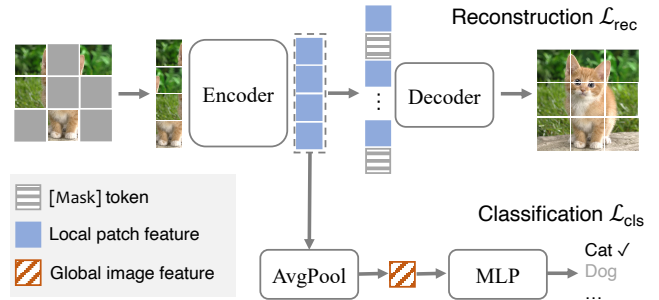


Figure 1: **Illustration of the proposed SupMAE method.** The proposed SupMAE extends MAE by adding a branch for supervised classification in parallel with the existing reconstruction objective. In the pre-training phase, only a subset of the visible patches is processed by a ViT encoder. Their corresponding patch features are used to (1) reconstruct the missing pixels and (2) classify the category. In the fine-tuning phase, the encoder is applied to uncorrupted images for recognition tasks.

MAE requires thousands of epochs to pre-train. This is because the key ingredient of MAE, Masked Image Modeling (MIM), only learns better middle-level interactions among patches (Li et al. 2022b). No global features, *i.e.*, features that can represent the entire image, are learned during pre-training.

How can we incorporate global feature learning into MAE? A natural solution is to leverage the golden labels, which allows MAE to know what concept it is reconstructing. However, whether the use of supervised labels would benefit MAE has not been explored yet. He et al. (2021) show that standard supervised pre-training underperforms even with more data augmentations (Touvron et al. 2021) or stronger regularization (Steiner et al. 2021).

In this paper, we first show that supervised pre-training can benefit MAE in training efficiency, model robustness, and transfer learning ability. The proposed method, Supervised MAE (SupMAE), extends MAE by adding a branch for supervised classification in parallel with the existing reconstruction objective (depicted in Figure 1). Formally, the subset of visible patches is fed into the ViT encoder to obtain local patch features. For the reconstruction branch, patch

features and padded `mask` tokens are processed by a small decoder that reconstructs the original image. For the classification branch, an average pooling operator is applied on patch features to get the global image feature which an MLP follows for classification. During fine-tuning, we only use the ViT encoder for downstream recognition tasks.

Unlike standard supervised pre-training methods (Touvron et al. 2021; Steiner et al. 2021) that use all patch features (or the equivalent `class` token), SupMAE only uses a subset of the visible patches to do classification. This is mainly based on the intuition that images are highly spatially redundant: humans can easily recognize an image even with a partial observation (a subset of patches). This design also makes SupMAE more sample-efficient: we can compute loss over *all* input tokens during training rather than just the subset that is masked out¹. From the perspective of data augmentation, random masking can generate different training samples for each iteration, serving as a strong regularization during supervised pre-training.

Through empirical experiments, we demonstrate that: (1). SupMAE is training efficient. SupMAE ViT-B/16 achieves 83.6% accuracy when fine-tuned on ImageNet-1K using only 400 pre-training epochs, $3\times$ less compared with 1600 epochs of MAE. We further benchmark the wall-clock running time of different supervised and self-supervised pre-training methods on GPU, showing the effectiveness and efficiency of the proposed SupMAE. (2). SupMAE is more robust to natural corruption. Notably, our SupMAE outperforms the MAE counterpart by an average gain of 1.8% on the robustness benchmark containing four ImageNet variants. (3). SupMAE learns more transferable features. Few-shot linear probing and fine-tuning on 20 downstream classification datasets show the superior performance of SupMAE. Moreover, our fine-tuned ViT-B/16 model achieves 49.0% mIoU on the ADE20K semantic segmentation validation dataset, revealing that the supervised pre-training can benefit the dense downstream tasks as well.

To summarize, the contributions of our paper are three-fold:

- To the best of our knowledge, this is the first work to study whether supervised pre-training can benefit MAE. This is a direction that intuitively makes sense because golden labels allow MAE to know what concept it is reconstructing.
- The proposed SupMAE only uses a subset of the visible patches to do classification rather than standard supervised pre-training that uses all patches. This design also makes SupMAE more sample-efficient: we can utilize *all* input tokens during training rather than just the subset that is masked out.
- Through empirical experiments, we demonstrate SupMAE is more training efficient and it also learns more robust features and transferable features.

¹MAE only computes the loss on masked patches.

Related Work

Supervised vision transformers Transformers (Vaswani et al. 2017), a self-attention-based architecture that originated in Natural Language Processing (NLP), has emerged as an alternative to CNNs in CV. Due to the lack of inductive biases inherent to CNNs, the first Vision Transformers (ViT) proposed in Dosovitskiy et al. (2020) do not perform well when trained on the mid-scale dataset ImageNet. Researchers have proposed to design data augmentations (Touvron et al. 2021; Touvron, Cord, and Jégou 2022) or add more regularization (Steiner et al. 2021) to improve the generality of supervised ViT. The proposed SupMAE is a supervised pre-training method built upon the recently introduced MAE (He et al. 2021). Compared with the aforementioned supervised methods, SupMAE only uses a *subset of the visible patches* to do classification rather than all patches.

Masked image modeling (MIM) Generative pre-training, *e.g.*, BERT (Devlin et al. 2018) and GPT (Radford et al. 2018), has been a well-established paradigm in NLP. Recently, researchers have been trying to introduce generative pre-training into CV. The pioneering work iGPT (Chen et al. 2020) adopts GPT-type auto-regressive modeling that predicts following pixels auto-regressively. More work adopts BERT-type Masked Image modeling (MIM) as the pretext task: representations are learned through reconstructing the missing part in the image. The reconstruction objective can be raw pixels (He et al. 2021; Xie et al. 2021b), discrete visual tokens (Bao, Dong, and Wei 2021; Dong et al. 2021), low-level local features (Wei et al. 2021), or latent representations (Baeviski et al. 2022). The proposed SupMAE is built upon MAE, the representative of generative approaches.

Contrastive learning Another line of work for self-supervised visual representation learning is contrastive learning (Chen*, Xie*, and He 2021; Caron et al. 2021; Xie et al. 2021a; Assran et al. 2022) SupCon (Khosla et al. 2020) is most relevant to our work: it extends contrastive learning into the supervised setting while we extend MIM into the supervised setting.

Multi-objective pre-training Our work is also highly related to multi-objective pre-training, where the model is trained with multiple auxiliary tasks. Zhang, Lee, and Lee (2016); Le, Patterson, and White (2018) augments the supervised CNNs with unsupervised reconstruction objective. Our SupMAE shares the same spirit but differs from these classical methods in numerous ways. More recently, Repr (Wang et al. 2022) incorporates local feature learning into contrastive methods via reconstructive pre-training. CMAE (Huang et al. 2022) combines contrastive learning with MAE to further strengthen the representation. Different from them, SupMAE extends the MAE into a fully supervised setting to enable MAE to effectively learn global features from golden labels.

SupMAE Method

The overall framework of the proposed SupMAE is illustrated in Figure 1. SupMAE consists of three components: encoder, reconstruction decoder, and classification head.

There are two complementary objectives: the reconstruction objective and the supervised classification objective. Details are introduced as follows.

Algorithm 1: SupMAE: PyTorch-like pseudo code

```
# f_enc / f_dec: encoder / decoder
# f_cls: mlp classification head
# mask_r: mask ratio
# λ_rec, λ_cls: objective weights
# tau: temperature

for x, tgt in loader: # load a minibatch
    x = patch_emb(x) # embed patches
    x_v, x_m = masking(x, mask_r) # random
        split visible and masked patches
    q_v = f_enc(x_v) # local patch features
    logits = f_cls(q_v) # predicted labels
    k_m = f_dec(q_v) # reconstructed pixels
    loss = λ_rec * rec_loss(k_m, x_m) + λ_cls *
        cls_loss(logits, tgt)
    loss.backward()
    update() # optimizer update

def rec_loss(k, x): # reconstruction
    x = norm_pix(x) # normalize every patch
    loss = (k - x) ** 2 # compute MSE loss
        over masked patches
    return loss

def cls_loss(logits, tgt): # classification
    loss = CrossEntropyLoss(logits/tau, tgt)
    return loss
```

Notes: class and mask tokens as well as positional embeddings are omitted for simplicity. For more details, please refer to our whole code in the supplementary files.

Image masking and encoding Following Dosovitskiy et al. (2020), the input image $\mathbf{x} \in \mathbb{R}^{H \times W \times C}$ is first divided into several non-overlapping patches $\mathbf{x}_p \in \mathbb{R}^{N \times (P^2 \cdot C)}$, where (H, W, C) corresponds to the resolution and channels of the original image, (P, P) is the resolution of each patch and $N = HW/P^2$ is the number of non-overlapping patches. The patches are fed into a linear projection (a.k.a., PatchEmbed) to get patch embeddings. Following He et al. (2021), we mask a large portion of patches (e.g., 75%). We denote the visible patches and masked patches as \mathbf{x}^v and \mathbf{x}^m , respectively. The remaining visible patches \mathbf{x}^v are added to positional embeddings and then processed by a ViT encoder (Dosovitskiy et al. 2020) to get corresponding local patch features \mathbf{q}^v . The subset of the visible patch features \mathbf{q}^v is used for reconstruction and classification, introduced next.

Reconstruction branch Due to the random masking, the length of the visible patch features \mathbf{q}^v is shorter than the image patch length N . Thus, we pad patch features \mathbf{q}^v with mask tokens (Devlin et al. 2018) to generate a full set of features. Each mask token is a shared, learned vector that indicates the presence of a missing patch to be reconstructed. As in the encoding, this full set of features is added with positional embeddings and processed by a transformer-based decoder. We find that the decoder of SupMAE can be very

light-weight, e.g., a one-layer transformer, which is consistent with the findings in MAE. After the decoding, a linear layer (omitted in Figure 1) projects features into the pixel space. The reconstruction objective \mathcal{L}_{rec} , mean squared error (MSE) in our SupMAE, is operated between the reconstructed and original images. Following prior work (He et al. 2021; Devlin et al. 2018), we compute the loss only on masked patches.

Classification branch The same set of visible patch features \mathbf{q}^v are further used for supervised classification. This is different from standard supervised pre-training, where all patches are used. More formally, a global pooling first condenses local patch features into the global representation of the image. The global representation is then used to predict the golden labels. The classification branch is complementary to the reconstruction branch from two perspectives: (1) the classification branch brings global feature learning into the framework, (2) we can compute loss over *all* input tokens during training rather than just the subset that is masked out (where reconstruction operates on).

For the classification head, we use a two-layer MLP, with Batchnorm (Ioffe and Szegedy 2015) and ReLU activation function injected in between. We further ablate the number of linear layers in Table 5f. We find it is also beneficial to introduce temperature τ (Hinton et al. 2015) as a parameter after the prediction of classification head (a.k.a. logits). The temperature τ is a parameter that controls the concentration level of the distribution, which is widely used in supervised (Wang et al. 2017)/self-supervised (Wu et al. 2018; Chen*, Xie*, and He 2021) feature learning. τ is set to 10 in our experiments. The classification loss \mathcal{L}_{cls} , cross-entropy (CE) in our SupMAE, is performed between predicted and golden labels. An alternative to representing the entire image is the class token, which is left 'untouched' during pre-training. Through empirical study, we find that global pooling brings better results than the class token (see Table 5b).

Overall objective Our SupMAE is optimized with reconstruction loss and classification loss, which simultaneously learns fine-grained local and global features. We use a weighted sum of these two loss functions as our overall loss as follows:

$$\mathcal{L} = \lambda_{rec} \mathcal{L}_{rec} + \lambda_{cls} \mathcal{L}_{cls} \quad (1)$$

where $\lambda_{rec}, \lambda_{cls}$ are weights to balance the two objectives. $\lambda_{rec}, \lambda_{cls}$ are set as 1.0 and 0.01, respectively (see Table 5d).

We further show the Pytorch-like pseudo-code in Algorithm 1. Please refer to our whole code in the supplementary files for more details.

Fine-tuning on downstream tasks After pre-training, our SupMAE model can be further fine-tuned on target recognition tasks to achieve better performance. During fine-tuning, we only keep the encoder while discarding the decoder and classification head. We use the full set of patches, i.e., uncorrupted images when fine-tuning downstream recognition tasks.

Table 1: **Comparison with supervised and self-supervised pre-training methods** All methods are using ViT-B/16 model. Besides the number of pre-training (PT) and fine-tuning (FT) epoch, we further estimate the wall-clock time for PT and FT, benchmarked on 8 A5000 GPUs. The normalized cost is relative to SupMAE. SupMAE shows a great efficiency and can achieve the same accuracy as MAE using only 30% compute.

method	PT epochs	PT cost (Hours)	FT epochs	FT cost (Hours)	Total cost (Hours)	Normalized cost	Top1 acc.
<i>Self-Supervised pre-training methods.</i>							
MoCov3 (Chen*, Xie*, and He 2021)	300	250	150	45.7	295.7	2.35×	83.2
BEiT (Bao, Dong, and Wei 2021)	800	233.3	100	31.5	264.8	2.10×	83.2
MAE (He et al. 2021)	1600	364	100	30	394	3.12×	83.6
<i>Supervised pre-training methods.</i>							
ViT (Dosovitskiy et al. 2020)	-	-	-	-	-	-	77.9
DeiT (Touvron et al. 2021)	300	91.5	-	-	91.5	0.73×	81.8
Naive supervised (He et al. 2021)	300	90	-	-	90	0.71×	82.3
SupMAE(Ours)	400	95.9	100	30	125.9	1×	83.6

Experimental Results

Main results on ImageNet-1K

We first conduct our experiments on widely used ImageNet-1K dataset (Deng et al. 2009). We basically follow MAE (He et al. 2021) for the setup and training hyper-parameters. Details are in our supplementary files.

Comparison with other pre-training methods We compare our SupMAE with other supervised or self-supervised pre-training methods in Table 1. All methods use the same ViT-B/16 architecture. For MAE and our SupMAE, the decoder is a one-layer transformer, and the mask ratio is set to 75%. The number of epochs is most widely used as an indicator of the training cost. However, it might be misleading as different methods require different time to run one epoch. Thus, we further benchmark the real wall-clock time of pre-training (PT) and fine-tuning (FT) on 8 NVIDIA A5000 24 GB GPU server with Pytorch. We use the official repository of MocoV3, DeiT, BEiT, and MAE to estimate the cost. Interestingly, we observe that the one-epoch cost of different methods varies greatly. The one-epoch cost of SupMAE is only $\sim 30\%$ of MoCov3 (Chen*, Xie*, and He 2021) because SupMAE’s encoder only processes a small subset of tokens. We also observe that data loading time is relatively negligible; most of the cost is computing.

We compare SupMAE with three supervised counterparts: ViT (Dosovitskiy et al. 2020), DeiT (Touvron et al. 2021) and naive supervised results from He et al. (2021). SupMAE can achieve 83.6% ImageNet top1 accuracy, significantly outperforming the standard supervised methods. When compared with the self-supervised method, such as MoCo-v3 (Chen*, Xie*, and He 2021), BEiT (Bao, Dong, and Wei 2021) and MAE (He et al. 2021), SupMAE can achieve comparable results with much lower training compute. This shows that supervised pre-training is compatible with self-supervised objectives and can improve the training efficiency of self-supervised methods. The efficiency and effectiveness of SupMAE lie on two facts: (1) the reconstruction objective helps to learn better local features (2) the classification objective provides the global feature learning ability.

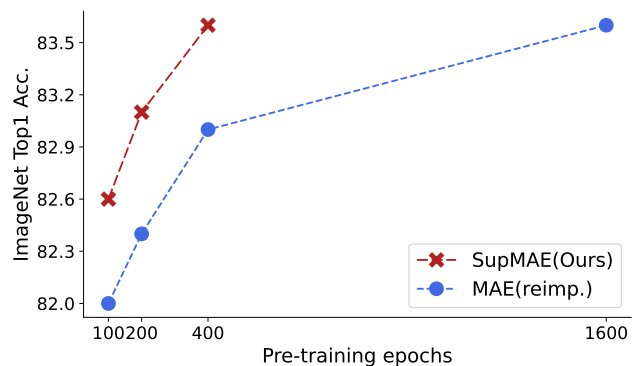


Figure 2: **Performance of different pre-training epochs** Comparison between MAE and SupMAE when pre-trained for different epochs. SupMAE is efficient and shows a much faster convergence speed.

Different pre-training epochs We compare different pre-training epochs of MAE and our proposed SupMAE in Figure 2. The encoder is ViT-B/16 architecture, and the mask ratio is set to 75%. We use a one-layer transformer decoder for SupMAE, unlike an 8-layer transformer decoder for MAE (He et al. 2021). We only change the number of pre-training epochs, *i.e.*, all models are fine-tuned for 100 epochs. When pre-trained for very few epochs, such as 100 epochs, SupMAE can achieve 82.6% accuracy, which is 0.6% higher than the MAE counterpart. When pre-trained for 200 epochs, SupMAE achieves 83.1% accuracy, higher than directly training from scratch 82.3% with 14% less time cost (78h vs. Naive supervised’s 90h). Our SupMAE can achieve 83.6% accuracy with only 400 pre-training epochs, while the MAE counterpart needs 1600 epochs to achieve such performance.

Unfortunately, we do not observe further improvement when we pre-train our SupMAE longer, such as for 800 epochs. Pre-training 800 epochs yields almost the same accuracy as 400 epochs. We conjecture there might be two reasons: (1) SupMAE can be categorized into supervised pre-training. However, supervised pre-training is easy to saturate, *e.g.*, DeiT (Touvron et al. 2021) saturates at 300 epochs even with a strong augmentation. The proposed SupMAE is

Table 2: **Robustness evaluation on robustness benchmark.** All methods use the same ViT-B/16 architecture. The metric is top-1 accuracy, except for IN-Corruption (Hendrycks and Dietterich 2019) which uses mean corruption error. We test the same SupMAE model as in Tabel 1 on 4 ImageNet variants *without* any specialized fine-tuning. The score is measured by the averaging metric across four variants (we use '100 - error' for the IN-Corruption performance metric). DeiT results are reproduced using the official checkpoint. Our SupMAE model shows better robustness on the benchmark.

dataset	MAE	DeiT	SupMAE(Ours)
IN-Corruption ↓	51.7	47.4	48.1
IN-Adversarial	35.9	27.9	35.5
IN-Rendition	48.3	45.3	51.0
IN-Sketch	34.5	32.0	36.0
Score	41.8	39.5	43.6

also suffering from this problem. (2) The fine-tuning recipe is relatively mature, and we might already exploit most of the information in ImageNet with the ViT-B/16 model. Since we follow almost all hyperparameters of MAE, we conjecture more dedicated hyperparameter tuning might lead to better results.

Robustness evaluation on ImageNet variants

In this section, we compare the robustness performance of MAE (He et al. 2021), DeiT (Touvron et al. 2021) and our SupMAE on four ImageNet variants. These datasets compare the robustness from different perspectives, including (1) IN-Corruption (Hendrycks and Dietterich 2019) for common corruptions (2) IN-Rendition (Hendrycks et al. 2021a) for semantic shifts (3) IN-Adversarial (Hendrycks et al. 2021b) for natural adversarial examples and (4) IN-Sketch (Wang et al. 2019) for color and texture shifts.

We test the same SupMAE model as in Table 1 on these ImageNet variants without any specialized fine-tuning. The results are summarized in Table 2. Our SupMAE significantly outperforms MAE in three out of four datasets. To further validate the average robustness, we further benchmark the robustness score, which is an average score across four datasets. Since the IN-Corruption uses mean corruption error, we use '100 - error' as its metric when averaging the score. As we can see, SupMAE achieves a 43.6% average score, which significantly outperforms self-supervised MAE (+1.8%) and supervised DeiT (+4.2%).

Transfer Learning experiments

Few-shot learning on 20 classification datasets We adopt the ELEVATOR (Li et al. 2022a) benchmark to conduct few-shot transfer learning on 20 image classification datasets. Table 3 reports the averaged accuracy of three methods: MAE, MoCo-v3, and the proposed SupMAE. More details about the datasets and breakdown results can be found in supplementary files. For a fair comparison, all the models use the same automatic hyper-parameter tuning process as in Li et al. (2022a), and no model-/dataset-specific

Table 3: **Few-shot transfer learning.** All methods use the same ViT-B/16 architecture. We report the linear probing and fine-tuning averaged scores on 20 image classification datasets. X-shot denotes the number of labeled images per category used during transfer learning. Our SupMAE significantly outperforms its MAE counterpart. MAE and MoCo-v3 results are from Li et al. (2022a).

Pre-training Settings		20 Image Classification Datasets		
Checkpoint	Method	5-shot	20-shot	50-shot
Linear Probing				
MAE	Self-Sup.	33.37 ± 1.98	48.03 ± 2.70	58.26 ± 0.84
MoCo-v3	Self-Sup.	50.17 ± 3.43	61.99 ± 2.51	69.71 ± 1.03
SupMAE(Ours)	Sup.	47.97 ± 0.44	60.86 ± 0.31	66.68 ± 0.47
Fine-tuning				
MAE	Self-Sup.	36.10 ± 3.25	54.13 ± 3.86	65.86 ± 2.42
MoCo-v3	Self-Sup.	39.30 ± 3.84	58.75 ± 5.55	70.33 ± 1.64
SupMAE(Ours)	Sup.	46.76 ± 0.12	64.61 ± 0.82	71.71 ± 0.66

Table 4: **Transferring to semantic segmentation on ADE20K** All methods use UperNet with ViT-B/16 backbone. For a fair comparison with supervised methods, we use a fine-tuned model for MAE and SupMAE. Naive supervised results are from He et al. (2021). MAE results are reproduced using the official fine-tuned checkpoint.

method	mIoU	aAcc	mAcc
Naive supervised	47.4	-	-
MAE	48.6	82.8	59.4
SupMAE (ours)	49.0	82.7	60.2

hyper-parameter tuning is employed. The average accuracy can represent the model transferability under a few-shot setting.

We observe that MAE performs worst under both linear probing and fine-tuning scenarios. We conjecture that this is caused by the fact that MAE can learn good local features but lacks the global image understanding. Our SupMAE performs significantly better than its MAE counterpart, thanks to the introduced global feature learning during pre-training. Under an extreme 5-shot linear probing setting, SupMAE outperforms its MAE counterpart by a large +14.6% margin. Our SupMAE shows better performance when we fine-tune the model end-to-end. We conjecture that this is because SupMAE only observe some fragments of images, *e.g.*, 25%, during the pre-training. End-to-end fine-tuning can adapt the model weights to suit the complete images better. Notably, SupMAE can outperform MoCo-v3 by a considerable +1.4% margin under 50-shot fine-tuning setting.

Semantic segmentation in ADE20k We adopt the UperNet (Xiao et al. 2018) as the semantic segmentation model on challenging ADE-20k (Zhou et al. 2019) dataset. For a fair comparison, we follow the same training configuration and code as MAE (He et al. 2021) with the MMSegmentation (MMSegmentation 2020) framework. The models are trained on 8 GPUs with a total batch size of 16 for 160k iterations. The input resolution is set to 512×512.

Table 5: **SupMAE ablation experiments** All experiments are using ViT-B/16 on ImageNet-1K. We report fine-tuning (ft) and linear probing (lin) accuracy (%). If not specified, the default is: the loss ratios of reconstruction (rec) and classification (cls) are 1 and 0.01, global pooling feature is used for classification, the decoder has depth 8, the data augmentation is random resized cropping, the masking ratio is 75%, and the pre-training length is 200 epochs. Default settings are marked in **gray**.

(a) **Pre-training objectives.** Reconstruction and classification supports each other.

rec	cls	ft	lin
✓		82.4	58.0
	✓	79.9	59.9
✓	✓	83.1	70.1

(b) **Class token.** Global pooling feature performs better than the additional `class` token.

case	ft	lin
cls token	79.1	65.8
global pool	83.1	70.1

(c) **Data augmentation.** Our SupMAE works with minimal data augmentation like MAE.

data aug	ft	lin
randcrop	83.1	70.1
randcrop,cjit	83.0	70.3

(d) **Loss ratio.** Small classification loss ratio works best.

cls ratio	ft	lin
0.02	82.9	70.2
0.01	83.1	70.1
0.005	83.1	69.8
0.002	82.8	68.8

(e) **Decoder depth.** SupMAE works well with a light decoder, *i.e.*, an one-layer transformer decoder.

blocks	ft	lin
1	83.1	65.7
4	83.1	68.2
8	83.1	70.1

(f) **MLP layers.** An appropriate number of layers should be set for the classification head.

mlp layers	ft	lin
1	83.0	72.5
2	83.1	70.1
3	82.9	69.5

We compare three methods in Table 4: naive supervised, MAE, and the proposed SupMAE. Naive supervised indicates the supervised pre-training done from scratch, in which we directly use the reported mIoU from He et al. (2021). We initialized the segmentation models using model weights after supervised fine-tuning on ImageNet-1K for two reasons: (1) it is a fair comparison with supervised methods (2) supervised fine-tuned weights can bring superior performance than the self-supervised pre-trained weights. Our SupMAE outperforms its MAE counterpart by a considerable +0.4% margin, showing that the supervised pre-training can benefit the dense downstream tasks as well

Ablation studies

To verify the components in the proposed SupMAE, we further conduct ablation studies using the default settings in Table 5 (see caption).

Pre-training objectives. Table 5a studies the pre-training objectives. As depicted in Figure 1, the method degrades into MAE with only the reconstruction (rec) objective. If we only use the classification (cls) objective, the method degrades into standard supervised pre-training (with 75% input patches masked out). We find that neither the reconstruction nor the classification objective can perform well when used in isolation. This is because only with both objectives can 100% patches be exploited: (1) reconstruction operates on 75% masked patches, and (2) classification operates on 25% visible patches.

Class token. Table 5b shows the impact of using the `class` token during pre-training. As introduced in ViT (Dosovitskiy et al. 2020), the additional `class` token is broadly viewed as the representation of the entire image. However, we find it better to use the global pooling feature (pooling over patch features) rather than `class` token in SupMAE. We conjecture that the `class` token may not work well when only operating on a subset of visible patches.

Data augmentation. Table 5c shows the influence of the data augmentation. Unlike other supervised pre-training methods, such as DeiT, which use a very heavy data augmentation, we find our SupMAE works pretty well with a minimal augmentation, *e.g.*, random resized cropping (randcrop). Adding color jittering (cjit) does not bring further improvements. This finding is consistent with MAE. This is because random masking already generates different training samples for each iteration. Thus, less data augmentation is required to regularize training.

Loss ratio. Table 5d studies different ratios of classification (cls) loss. To balance two pre-training objectives (see Equation 1), we first fix the ratio of reconstruction loss to 1, and then we tune the classification ratio. We find that a small classification loss ratio works best. Too large a ratio forces SupMAE to degrade into standard supervised pre-training, which hurts performance (see Table 5a).

Decoder depth. Table 5e studies different depths of the decoder. As we increase the depth of the decoder, the linear probing (lin) accuracy increases steadily, but the end-to-end fine-tuning (ft) accuracy stays the same. The finding is also consistent with MAE. This is due to the gap between pixel reconstruction and classification: a shallow decoder would require the output of the encoder to be more specialized for reconstruction, which is harmful to linear probing.

MLP layers. Table 5f shows the influence of the number of MLP layers in the classification head. Increasing the layers decreases the linear probing (lin) accuracy. We conjecture that this is because one linear layer makes the encoder output linearly separable, which is suitable for linear probing. However, since SupMAE has a reconstruction objective, we may want the latent representations at a more abstract level. Thus, we choose a two-layer MLP as default setting.

Discussion

ImageNet accuracy of pre-training Since our SupMAE is pre-trained in a supervised fashion on ImageNet, the pre-

Table 6: **ImageNet-1K accuracy of pre-training** We report the ImageNet accuracy of pre-trained (PT) and fine-tuned (FT) SupMAE model on ImageNet-1K. All models are from Table 1. (25%) represents using 25% patches for inference. Results show that even without fine-tuning, the pre-trained SupMAE model can achieve some level of accuracy on ImageNet-1K.

	PT (25%)	PT (100%)	FT
Top1 acc.	66.0	68.9	83.6

trained model can directly perform inference on the ImageNet dataset. We show the resulting performance in Table 6. The pre-trained (PT) and fine-tuned (FT) models are from Table 1. For the PT model, we test with two different patch ratios. When we keep the same ratio as for pre-training, *i.e.*, 25%, we achieve 66.0% top1 accuracy. Interestingly, if we use all patches for inference, we can achieve an even higher accuracy of 68.9%. This shows that the pre-trained SupMAE model can achieve some level of accuracy even without fine-tuning. It is worth noting that we do not expect the PT model to perform as well as the FT model. Table 1 demonstrates that the pre-trained SupMAE model can provide a good initial representation point for other tasks.

ImageNet accuracy curve during fine-tuning We further report the per epoch ImageNet accuracy during fine-tuning in Figure 3. MAE and SupMAE use ViT-B/16, and the models are pre-trained for 200 epochs. Following the fine-tuning recipe in He et al. (2021), the pre-trained models are further fine-tuned on ImageNet for 100 epochs. We can see that SupMAE can achieve very high accuracy even at the first epoch. This is because our SupMAE can learn a good global feature via the supervised branch, which brings a better initialization point for fine-tuning. Thanks to the good initialization, SupMAE can significantly improve over MAE when we only have a few samples in downstream datasets (See few-shot learning experiments in Table 3).

Transfer to SimMIM Our introduced supervised branch is also supposed to be compatible with other self-supervised MIM methods. To further validate the transferability, we extend the SimMIM (Xie et al. 2021b) into a fully-supervised setting, like we do to MAE. SimMIM predicts raw pixel values of the randomly masked patches by a lightweight one-layer head and performs learning using a simple L_1 loss. The major difference between MAE and SimMIM is the input of the encoder. SimMIM uses the corrupted image, where the masked patches are replaced by `mask` tokens (but it is still a complete image), while MAE only uses the visible patches as input. When we extend the SimMIM, we only use the visible patch features to generate global features, the same as SupMAE.

We validate our approach using the Swin-Base (Liu et al. 2021) model to show that the supervised branch is also compatible with the hierarchical transformer. We set the loss ratio of the supervised classification branch as 0.01, the same as SupMAE. All other training hyperparameters are the same as SimMIM. We pre-train the models for 100

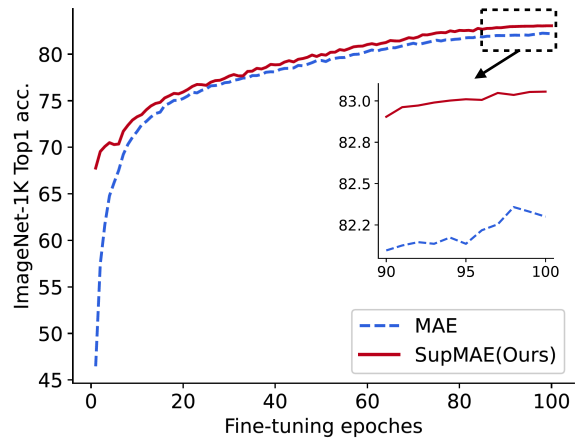


Figure 3: Comparison between MAE and SupMAE when fine-tuned for 100 epochs on ImageNet-1K. The model architecture is ViT-B/16. Both MAE and SupMAE are pre-trained for 200 epochs. Our SupMAE brings a much better initialization point than its MAE counterpart.

Table 7: **Integrating the supervised branch into SimMIM** The model is Swin-Base. The pre-training and fine-tuning resolutions are all set to 192×192 . Results show that the supervised branch is also compatible with other MIM frameworks.

method	SimMIM	SimMIM w/ sup.
Top1 acc.	82.8	83.0

epochs and then fine-tune them for another 100 epochs. The input resolutions are set as 192×192 . The supervised branch can bring an additional +0.2% improvement over the vanilla SimMIM. It is worth noting that we do not do any hyperparameters tuning over SimMIM; more improvement can be expected if more careful tuning is done.

Conclusion

In this paper, we propose Supervised Masked Autoencoders (SupMAE), a *fully-supervised* extension of MAE obtained by adding a supervised classification branch. The supervised pre-training enables MAE to learn global features from golden labels effectively. Unlike the standard supervised pre-training where all image patches are used, the proposed SupMAE only exploits a visible subset of image patches for classification. Through thorough experiments, we demonstrate that SupMAE is more training efficient and learns more robust and transferable features.

SupMAE is a hybrid pre-training method with external label supervision and self-provided supervision. We believe that our method can shed light on future research on pre-training with multiple objectives.

Acknowledgment

This work was supported in part by NSF CCF Grant No. 2107085 ,ONR Minerva program, iMAGiNE - the Intelligent Machine Engineering Consortium at UT Austin, and a UT Cockrell School of Engineering Doctoral Fellowship.

Appendix

Implementation details on ImageNet

We follow the hyperparameters in MAE (He et al. 2021).

Pre-training. The pre-training setting is in Table 8. We train our SupMAE for 400 epochs with 20 epochs warm-up. The models are trained in a distributed fashion on 16 GPUs with a total batch size of 4096 (256 for each GPU). Like in MAE, we use the linear lr scaling rule: $lr = base_lr \times batchsize / 256$.

Table 8: Pre-training hyperparameters.

config	value
optimizer	AdamW
base learning rate	1.5e-4
weight decay	0.05
optimizer momentum	$\beta_1, \beta_2=0.9, 0.95$
batch size	4096
GPU number	16
learning rate schedule	cosine decay
pre-training epochs	400
warmup epochs	20
augmentation	RandomResizedCrop

End-to-end fine-tuning. The fine-tuning setting is in Table 9. Like in MAE, we use the global pooling feature rather than `class` token during fine-tuning. The models are fine-tuned on 8 GPUs with a total batch size of 1024 (128 for each GPU). Like in the pre-training, we use the linear lr scaling rule: $lr = base_lr \times batchsize / 256$.

Linear probing. The linear probing setting is in Table 10. Like MAE, we use the `class` token during linear probing. The models are trained on 8 GPUs with a total batch size of 8192 (1024 for each GPU) with a LARS optimizer. A larger base lr is used in linear probing.

Implementation details of few-shot learning

We follow the few-shot transfer learning toolkit in ELEVATER (Li et al. 2022a)².

Datasets

As summarized in Table 11, ELEVATER (Li et al. 2022a) contains 20 image classification datasets, spans from common objects (Krizhevsky, Hinton et al. 2009; Everingham et al. 2010), numerical digits (Deng 2012), aircraft images (Maji et al. 2013), satellite images (Helber et al. 2019) and so on. We use the data samples defined in the ELEVATER toolkit when we perform few-shot learning.

²https://github.com/Computer-Vision-in-the-Wild/Elevater_Toolkit.IC

Table 9: End-to-end fine-tuning hyperparameters.

config	value
optimizer	AdamW
base learning rate	1e-3
weight decay	0.05
optimizer momentum	$\beta_1, \beta_2=0.9, 0.999$
layer-wise lr decay	0.65
batch size	1024
learning rate schedule	cosine decay
warmup epochs	5
training epochs	100
augmentation	RandAug (9, 0.5)
label smoothing	0.1
reprob	0.25
mixup	0.8
cutmix	1.0
drop path	0.1

Table 10: Linear probing hyperparameters.

config	value
optimizer	LARS
base learning rate	0.1
weight decay	0
optimizer momentum	0.9
batch size	8192
learning rate schedule	cosine decay
warmup epochs	10
training epochs	90
augmentation	RandomResizedCrop

Automatic hyperparameter tuning We also follow the automatic hyperparameter tuning strategy in the ELEVATER toolkit. We split its training set into training (80%) and validation (20%) sets for each setting. We will ensure that each category has at least one training sample. For each setting, we first grid search the optimal learning rate η and weight decay α . In the hyper-parameter search phase, each configuration (η, α) will run for 10 epochs. After obtaining the optimal (η, α) , the final model will be trained for 50 epochs and tested on the testing set.

Results breakdown We further report the results of each dataset and setting in Table 12. The MAE and MoCo-v3 results are from Li et al. (2022a). We note that our SupMAE model uses global pooling to extract global features in linear probing rather than the `class` token used by MAE and MoCo-v3. This is because our SupMAE model is pre-trained with global pool mode. For fine-tuning, all methods use global pooling. Our SupMAE outperforms its MAE counterparts by a large margin, *e.g.*, +14.5% average score for 5-shot learning probing. SupMAE shows more advantage under end-to-end fine-tuning setting, achieving 13 best accuracies among 20 datasets for 50-shot fine-tuning.

Table 11: Statistics of 20 image classification datasets in ELEVATER (Li et al. 2022a).

Dataset	#Concepts	Train size	Test size	Evaluation metric	Source
Hateful Memes (Kiela et al. 2020)	2	8,500	500	ROC AUC	Facebook
PatchCamelyon (Veeling et al. 2018)	2	262,144	32,768	Accuracy	Tensorflow
Rendered-SST2 (Radford et al. 2021)	2	6,920	1,821	Accuracy	OpenAI
KITTI Distance (Fritsch, Kuehnl, and Geiger 2013)	4	6,347	711	Accuracy	KITTI website
FER 2013 (kaggle 2013)	7	28,709	3,589	Accuracy	Kaggle fer2013
CIFAR-10 (Krizhevsky, Hinton et al. 2009)	10	50,000	10,000	Accuracy	Tensorflow
EuroSAT (Helber et al. 2019)	10	5,000	5,000	Accuracy	Tensorflow
MNIST (Deng 2012)	10	60,000	10,000	Accuracy	Tensorflow
VOC 2007 Classification (Everingham et al. 2010)	20	2,501	4,952	11-point mAP	VOC 2007
Oxford-IIIT Pets (Parkhi et al. 2012)	37	3,680	3,669	Mean-per-class	Oxford-IIIT Pets
GTSRB (Stallkamp et al. 2011)	43	26,640	12,630	Accuracy	GTSRB website
Resisc-45 (Cheng, Han, and Lu 2017)	45	3,150	25,200	Accuracy	Tensorflow
Describable Textures (Cimpoi et al. 2014)	47	1,880	1,880	Accuracy	DTD website
CIFAR-100 (Krizhevsky, Hinton et al. 2009)	100	50,000	10,000	Accuracy	Tensorflow
FGVC Aircraft (variants) (Maji et al. 2013)	100	3,334	3,333	Mean-per-class	FGVC website
Food-101 (Bossard, Guillaumin, and Gool 2014)	101	75,750	25,250	Accuracy	Tensorflow
Caltech-101 (Fei-Fei, Fergus, and Perona 2004)	102	3,060	6,084	Mean-per-class	Tensorflow
Oxford Flowers 102 (Nilsback and Zisserman 2008)	102	1,020	6,149	Mean-per-class	Tensorflow
Stanford Cars (Krause et al. 2013)	196	8,144	8,041	Accuracy	Stanford Cars
Country-211 (Radford et al. 2021)	211	31,650	21,100	Accuracy	OpenAI
Total	1151	638429	192677	-	-

Table 12: Breakdown results of few-shot learning on 20 classification datasets.

Ckpt.	Shot	Score																				
			Caltech101	CIFAR10	CIFAR100	Country211	DTD	EuroSat	FER2013	FGVCAircraft	Food101	GTSRB	HatefulMemes	KittiDistance	MNIST	Flowers102	OxfordPets	PatchCamelyon	SST2	RESISC45	StanfordCars	VOC2007
Linear Probing																						
MAE	5	33.4	59.0	34.0	21.2	2.8	35.0	64.4	21.3	7.0	7.7	17.5	51.4	46.1	63.4	50.9	17.2	54.9	50.1	38.9	6.3	18.3
	20	48.0	85.5	44.9	43.5	4.4	58.3	74.1	23.5	29.9	30.4	41.1	51.7	49.8	52.9	71.9	60.0	52.7	53.2	67.4	25.5	39.9
	50	58.3	88.7	67.3	53.3	6.9	66.0	86.4	27.1	39.2	42.8	57.0	50.8	54.0	81.5	71.9	76.5	69.4	51.6	78.6	36.7	59.2
MoCo-v3	5	50.2	80.8	78.5	60.5	4.8	57.1	77.1	20.5	11.8	36.6	31.4	50.7	46.7	64.1	79.5	76.2	54.7	50.0	61.9	13.4	47.9
	20	62.0	91.3	67.7	75.5	7.6	66.3	84.8	30.9	38.2	59.3	53.9	53.5	48.5	81.8	89.5	86.4	52.1	51.6	77.3	49.5	74.2
	50	69.7	92.1	93.6	79.0	10.3	73.4	92.3	40.2	48.0	66.8	66.7	50.3	60.5	88.3	89.5	90.2	75.1	51.3	84.1	63.1	79.2
SupMAE (Ours)	5	48.0	73.9	55.1	38.5	4.4	44.4	77.0	19.2	16.2	33.8	31.1	47.2	42.8	73.3	82.7	72.0	66.8	50.4	61.9	16.7	52.2
	20	60.9	87.6	70.6	54.5	7.3	61.7	89.7	23.8	33.2	53.6	55.9	50.0	57.2	87.6	90.5	85.4	76.1	51.1	76.2	36.2	69.3
	50	66.7	88.5	80.1	65.6	10.0	68.0	92.1	34.9	40.3	62.3	64.2	50.7	61.6	94.3	90.5	88.7	80.4	52.5	84.4	48.3	76.2
Fine-tuning																						
MAE	5	36.1	70.8	34.4	13.1	2.1	41.4	64.1	20.8	8.2	13.3	14.8	49.6	38.0	46.8	68.8	37.8	53.3	50.9	50.4	6.0	37.4
	20	54.1	91.0	50.1	40.4	3.6	59.7	79.5	22.6	32.5	22.4	62.2	54.8	46.0	90.9	81.6	78.0	67.7	51.7	65.5	21.6	60.8
	50	65.9	92.9	71.5	54.7	4.9	66.2	87.8	34.1	42.8	51.9	95.6	51.3	50.1	96.1	81.6	84.8	77.3	52.4	85.2	68.0	68.0
MoCo-v3	5	39.3	73.7	70.3	17.4	2.3	45.6	60.0	13.5	7.2	27.6	16.5	50.8	43.5	18.1	65.7	77.1	50.9	50.7	58.2	11.2	25.7
	20	58.8	91.9	58.4	59.2	5.0	63.4	69.7	19.8	47.4	55.5	86.7	53.5	48.5	53.4	85.8	87.4	51.5	51.4	78.5	49.2	59.2
	50	70.3	92.8	89.1	77.5	6.9	71.3	92.6	31.0	53.4	63.2	96.5	50.9	57.3	94.3	85.8	90.2	74.2	50.4	87.3	66.2	75.7
SupMAE (Ours)	5	46.8	75.4	48.4	27.7	2.9	43.9	74.3	19.4	18.4	30.1	36.8	50.5	37.4	79.4	84.3	69.6	57.0	51.2	61.4	13.5	53.6
	20	64.6	92.9	64.4	60.7	4.6	61.9	86.7	27.2	44.5	56.3	90.6	52.0	51.1	87.9	90.2	88.3	72.9	51.1	81.4	59.1	68.4
	50	71.7	94.1	84.0	74.0	6.6	69.3	93.3	36.0	58.4	68.7	97.0	51.0	57.3	96.8	90.2	91.3	78.9	52.2	88.0	77.7	69.6

References

Assran, M.; Caron, M.; Misra, I.; Bojanowski, P.; Bordes, F.; Vincent, P.; Joulin, A.; Rabbat, M.; and Ballas, N. 2022. Masked Siamese Networks for Label-Efficient Learning. *arXiv preprint arXiv:2204.07141*.

Baevski, A.; Hsu, W.-N.; Xu, Q.; Babu, A.; Gu, J.; and Auli, M. 2022. Data2vec: A general framework for self-supervised learning in speech, vision and language. *arXiv preprint arXiv:2202.03555*.

Bao, H.; Dong, L.; and Wei, F. 2021. Beit: Bert pre-training of image transformers. *arXiv preprint arXiv:2106.08254*.

Bossard, L.; Guillaumin, M.; and Gool, L. V. 2014.

Food-101—mining discriminative components with random forests. In *ECCV*.

Caron, M.; Touvron, H.; Misra, I.; Jégou, H.; Mairal, J.; Bojanowski, P.; and Joulin, A. 2021. Emerging properties in self-supervised vision transformers. In *Proceedings of the IEEE/CVF International Conference on Computer Vision*, 9650–9660.

Chen, M.; Radford, A.; Child, R.; Wu, J.; Jun, H.; Luan, D.; and Sutskever, I. 2020. Generative pretraining from pixels. In *International conference on machine learning*, 1691–1703. PMLR.

Chen*, X.; Xie*, S.; and He, K. 2021. An Empirical Study

- of Training Self-Supervised Vision Transformers. *arXiv preprint arXiv:2104.02057*.
- Cheng, G.; Han, J.; and Lu, X. 2017. Remote sensing image scene classification: Benchmark and state of the art. *Proceedings of the IEEE*.
- Cimpoi, M.; Maji, S.; Kokkinos, I.; Mohamed, S.; and Vedaldi, A. 2014. Describing textures in the wild. In *CVPR*.
- Deng, J.; Dong, W.; Socher, R.; Li, L.-J.; Li, K.; and Fei-Fei, L. 2009. Imagenet: A large-scale hierarchical image database. In *2009 IEEE conference on computer vision and pattern recognition*, 248–255. Ieee.
- Deng, L. 2012. The MNIST database of handwritten digit images for machine learning research. *IEEE signal processing magazine*.
- Devlin, J.; Chang, M.-W.; Lee, K.; and Toutanova, K. 2018. Bert: Pre-training of deep bidirectional transformers for language understanding. *arXiv preprint arXiv:1810.04805*.
- Dong, X.; Bao, J.; Zhang, T.; Chen, D.; Zhang, W.; Yuan, L.; Chen, D.; Wen, F.; and Yu, N. 2021. Peco: Perceptual codebook for bert pre-training of vision transformers. *arXiv preprint arXiv:2111.12710*.
- Dosovitskiy, A.; Beyer, L.; Kolesnikov, A.; Weissenborn, D.; Zhai, X.; Unterthiner, T.; Dehghani, M.; Minderer, M.; Heigold, G.; Gelly, S.; et al. 2020. An image is worth 16x16 words: Transformers for image recognition at scale. *arXiv preprint arXiv:2010.11929*.
- Everingham, M.; Van Gool, L.; Williams, C. K.; Winn, J.; and Zisserman, A. 2010. The pascal visual object classes (VOC) challenge. *IJCV*.
- Fei-Fei, L.; Fergus, R.; and Perona, P. 2004. Learning generative visual models from few training examples: An incremental Bayesian approach tested on 101 object categories. In *CVPR workshop*.
- Fritsch, J.; Kuehnl, T.; and Geiger, A. 2013. A new performance measure and evaluation benchmark for road detection algorithms. In *ITSC*. IEEE.
- Girshick, R.; Donahue, J.; Darrell, T.; and Malik, J. 2014. Rich feature hierarchies for accurate object detection and semantic segmentation. In *Proceedings of the IEEE conference on computer vision and pattern recognition*, 580–587.
- He, K.; Chen, X.; Xie, S.; Li, Y.; Dollár, P.; and Girshick, R. 2021. Masked autoencoders are scalable vision learners. *arXiv preprint arXiv:2111.06377*.
- He, K.; Gkioxari, G.; Dollár, P.; and Girshick, R. 2017. Mask r-cnn. In *Proceedings of the IEEE international conference on computer vision*, 2961–2969.
- He, K.; Zhang, X.; Ren, S.; and Sun, J. 2016. Deep residual learning for image recognition. In *Proceedings of the IEEE conference on computer vision and pattern recognition*, 770–778.
- Helber, P.; Bischke, B.; Dengel, A.; and Borth, D. 2019. EuroSat: A novel dataset and deep learning benchmark for land use and land cover classification. *IEEE Journal of Selected Topics in Applied Earth Observations and Remote Sensing*.
- Hendrycks, D.; Basart, S.; Mu, N.; Kadavath, S.; Wang, F.; Dorundo, E.; Desai, R.; Zhu, T.; Parajuli, S.; Guo, M.; et al. 2021a. The many faces of robustness: A critical analysis of out-of-distribution generalization. In *Proceedings of the IEEE/CVF International Conference on Computer Vision*, 8340–8349.
- Hendrycks, D.; and Dietterich, T. 2019. Benchmarking neural network robustness to common corruptions and perturbations. *arXiv preprint arXiv:1903.12261*.
- Hendrycks, D.; Zhao, K.; Basart, S.; Steinhardt, J.; and Song, D. 2021b. Natural adversarial examples. In *Proceedings of the IEEE/CVF Conference on Computer Vision and Pattern Recognition*, 15262–15271.
- Hinton, G.; Vinyals, O.; Dean, J.; et al. 2015. Distilling the knowledge in a neural network. *arXiv preprint arXiv:1503.02531*, 2(7).
- Huang, Z.; Jin, X.; Lu, C.; Hou, Q.; Cheng, M.-M.; Fu, D.; Shen, X.; and Feng, J. 2022. Contrastive Masked Autoencoders are Stronger Vision Learners. *arXiv preprint arXiv:2207.13532*.
- Ioffe, S.; and Szegedy, C. 2015. Batch normalization: Accelerating deep network training by reducing internal covariate shift. In *International conference on machine learning*, 448–456. PMLR.
- kaggle. 2013. FER 2013: Kaggle challenges in representation learning facial expression recognition. <https://www.kaggle.com/>.
- Khosla, P.; Teterwak, P.; Wang, C.; Sarna, A.; Tian, Y.; Isola, P.; Maschinot, A.; Liu, C.; and Krishnan, D. 2020. Supervised contrastive learning. *Advances in Neural Information Processing Systems*, 33: 18661–18673.
- Kiela, D.; Firooz, H.; Mohan, A.; Goswami, V.; Singh, A.; Ringshia, P.; and Testuggine, D. 2020. The hateful memes challenge: Detecting hate speech in multimodal memes. *NeurIPS*.
- Krause, J.; Stark, M.; Deng, J.; and Fei-Fei, L. 2013. 3d object representations for fine-grained categorization. In *ICCV workshops*.
- Krizhevsky, A.; Hinton, G.; et al. 2009. Learning multiple layers of features from tiny images.
- Krizhevsky, A.; Sutskever, I.; and Hinton, G. E. 2012. Imagenet classification with deep convolutional neural networks. *Advances in neural information processing systems*, 25: 1097–1105.
- Le, L.; Patterson, A.; and White, M. 2018. Supervised autoencoders: Improving generalization performance with unsupervised regularizers. *Advances in neural information processing systems*, 31.
- Li, C.; Liu, H.; Li, L. H.; Zhang, P.; Aneja, J.; Yang, J.; Jin, P.; Lee, Y. J.; Hu, H.; Liu, Z.; et al. 2022a. ELEVATER: A Benchmark and Toolkit for Evaluating Language-Augmented Visual Models. *arXiv preprint arXiv:2204.08790*.
- Li, S.; Wu, D.; Wu, F.; Zang, Z.; Wang, K.; Shang, L.; Sun, B.; Li, H.; Li, S.; et al. 2022b. Architecture-Agnostic Masked Image Modeling—From ViT back to CNN. *arXiv preprint arXiv:2205.13943*.

- Liu, Z.; Lin, Y.; Cao, Y.; Hu, H.; Wei, Y.; Zhang, Z.; Lin, S.; and Guo, B. 2021. Swin transformer: Hierarchical vision transformer using shifted windows. In *Proceedings of the IEEE/CVF International Conference on Computer Vision*, 10012–10022.
- Long, J.; Shelhamer, E.; and Darrell, T. 2015. Fully convolutional networks for semantic segmentation. In *Proceedings of the IEEE conference on computer vision and pattern recognition*, 3431–3440.
- Maji, S.; Rahtu, E.; Kannala, J.; Blaschko, M.; and Vedaldi, A. 2013. Fine-grained visual classification of aircraft. *arXiv preprint arXiv:1306.5151*.
- MMSegmentation, C. 2020. MMSegmentation: OpenMM-Lab Semantic Segmentation Toolbox and Benchmark. <https://github.com/open-mmlab/mms Segmentation>.
- Nilsback, M.-E.; and Zisserman, A. 2008. Automated flower classification over a large number of classes. In *Indian Conference on Computer Vision, Graphics & Image Processing*. IEEE.
- Parkhi, O. M.; Vedaldi, A.; Zisserman, A.; and Jawahar, C. 2012. Cats and dogs. In *CVPR*.
- Radford, A.; Kim, J. W.; Hallacy, C.; Ramesh, A.; Goh, G.; Agarwal, S.; Sastry, G.; Askell, A.; Mishkin, P.; Clark, J.; et al. 2021. Learning transferable visual models from natural language supervision. In *ICML*.
- Radford, A.; Narasimhan, K.; Salimans, T.; Sutskever, I.; et al. 2018. Improving language understanding by generative pre-training.
- Simonyan, K.; and Zisserman, A. 2014. Very deep convolutional networks for large-scale image recognition. *arXiv preprint arXiv:1409.1556*.
- Stallkamp, J.; Schlipsing, M.; Salmen, J.; and Igel, C. 2011. The German traffic sign recognition benchmark: a multi-class classification competition. In *IJCNN*.
- Steiner, A.; Kolesnikov, A.; Zhai, X.; Wightman, R.; Uszkoreit, J.; and Beyer, L. 2021. How to train your vit? data, augmentation, and regularization in vision transformers. *arXiv preprint arXiv:2106.10270*.
- Touvron, H.; Cord, M.; Douze, M.; Massa, F.; Sablayrolles, A.; and Jégou, H. 2021. Training data-efficient image transformers & distillation through attention. In *International Conference on Machine Learning*, 10347–10357. PMLR.
- Touvron, H.; Cord, M.; and Jégou, H. 2022. DeiT III: Revenge of the ViT. *arXiv preprint arXiv:2204.07118*.
- Vaswani, A.; Shazeer, N.; Parmar, N.; Uszkoreit, J.; Jones, L.; Gomez, A. N.; Kaiser, Ł.; and Polosukhin, I. 2017. Attention is all you need. *Advances in neural information processing systems*, 30.
- Veeling, B. S.; Linmans, J.; Winkens, J.; Cohen, T.; and Welling, M. 2018. Rotation equivariant CNNs for digital pathology. In *MICCAI*.
- Wang, F.; Xiang, X.; Cheng, J.; and Yuille, A. L. 2017. Normface: L2 hypersphere embedding for face verification. In *Proceedings of the 25th ACM international conference on Multimedia*, 1041–1049.
- Wang, H.; Ge, S.; Lipton, Z.; and Xing, E. P. 2019. Learning robust global representations by penalizing local predictive power. *Advances in Neural Information Processing Systems*, 32.
- Wang, L.; Liang, F.; Li, Y.; Ouyang, W.; Zhang, H.; and Shao, J. 2022. Repr: Improving self-supervised vision transformer with reconstructive pre-training. *arXiv preprint arXiv:2201.06857*.
- Wei, C.; Fan, H.; Xie, S.; Wu, C.-Y.; Yuille, A.; and Feichtenhofer, C. 2021. Masked Feature Prediction for Self-Supervised Visual Pre-Training. *arXiv preprint arXiv:2112.09133*.
- Wu, Z.; Xiong, Y.; Yu, S. X.; and Lin, D. 2018. Unsupervised feature learning via non-parametric instance discrimination. In *Proceedings of the IEEE conference on computer vision and pattern recognition*, 3733–3742.
- Xiao, T.; Liu, Y.; Zhou, B.; Jiang, Y.; and Sun, J. 2018. Unified perceptual parsing for scene understanding. In *Proceedings of the European conference on computer vision (ECCV)*, 418–434.
- Xie, Z.; Lin, Y.; Yao, Z.; Zhang, Z.; Dai, Q.; Cao, Y.; and Hu, H. 2021a. Self-supervised learning with swin transformers. *arXiv preprint arXiv:2105.04553*.
- Xie, Z.; Zhang, Z.; Cao, Y.; Lin, Y.; Bao, J.; Yao, Z.; Dai, Q.; and Hu, H. 2021b. Simmim: A simple framework for masked image modeling. *arXiv preprint arXiv:2111.09886*.
- Zhang, Y.; Lee, K.; and Lee, H. 2016. Augmenting supervised neural networks with unsupervised objectives for large-scale image classification. In *International conference on machine learning*, 612–621. PMLR.
- Zhou, B.; Zhao, H.; Puig, X.; Xiao, T.; Fidler, S.; Barriuso, A.; and Torralba, A. 2019. Semantic understanding of scenes through the ade20k dataset. *International Journal of Computer Vision*, 127(3): 302–321.